

Microfluidic Digital PCR Enables Multigene Analysis of Individual Environmental Bacteria

Elizabeth A. Ottesen,¹ Jong Wook Hong,² Stephen R. Quake,³ Jared R. Leadbetter^{4*}

Gene inventory and metagenomic techniques have allowed rapid exploration of bacterial diversity and the potential physiologies present within microbial communities. However, it remains nontrivial to discover the identities of environmental bacteria carrying two or more genes of interest. We have used microfluidic digital polymerase chain reaction (PCR) to amplify and analyze multiple, different genes obtained from single bacterial cells harvested from nature. A gene encoding a key enzyme involved in the mutualistic symbiosis occurring between termites and their gut microbiota was used as an experimental hook to discover the previously unknown ribosomal RNA-based species identity of several symbionts. The ability to systematically identify bacteria carrying a particular gene and to link any two or more genes of interest to single species residing in complex ecosystems opens up new opportunities for research on the environment.

A major challenge of environmental science is the identification of microbial species capable of catalyzing important activities in situ (1). PCR-based techniques that use single genes as proxies for organisms or key microbial activities continue to provide valuable insights into microbial community diversity (2–4). However, it has been difficult to interrelate gene inventories to derive correspondences between any two or more specific genes of interest, or to determine the phylogenetic species identity of organisms carrying particular genetic capabilities. Metagenomic (5) analyses of complex communities are dominated by genome “shrapnel”; unless the microbial community is dominated by one or a few species (6, 7), resident genomes are not reliably reconstructed via computation (8, 9). A gene of interest can be attributed to a specific organism only if it is linked to an unambiguous phylogenetic marker (i.e., on the same genome fragment) (5, 10). Both PCR and metagenomic studies are typically carried out on homogenized, whole-community genomic DNA preparations. Thus, the cell as a distinct informational entity is almost entirely lost.

Outside of traditional culture-based isolation, few approaches can attribute multiple genes to a single species or cell type. Microautoradiography (11) and stable isotope probing (12) allow detection of cells or retrieval of genetic material from organisms that use a substrate of interest, but these techniques require active cellular incorporation of that substrate. Microscopy-based in situ hybridization techniques [fluorescence in

situ hybridization (FISH) and variants (13, 14)] allow colocalization of sequences through probe hybridization, but these methods require that both genes be actively transcribed, that their sequences be known in advance, and that their difference from related, nontarget genes is sufficient to enable effective probe design and implementation. Single-cell whole-genome amplification has recently been reported for a highly abundant, culturable marine microbial species, but has not yet been shown to be scalable to interrogating multitudes of diverse, co-resident microbes (15). Here, we applied commercially available microfluidic devices to perform a variant of “digital PCR” (16), separating and interrogating hundreds of individual environmental bacteria in parallel.

Microfluidic devices allow control and manipulation of small volumes of liquid (17, 18), in this case allowing for rapid separation and partitioning of single cells from a complex parent sample. Single, partitioned cells served as templates for individual multiplex PCR reactions using primers and probes for simultaneous amplification of both small-subunit ribosomal RNA (rRNA) and metabolic genes of interest. Primers and probes with broad target specificities were used, with subsequent resolution of exact gene sequences after successful amplification and retrieval. This technique operates independent of gene expression, position on the genome, or physiological state of the cell at the time of harvest. The result was rapid colocalization of two genes (encoding 16S rRNA and a key metabolic enzyme) to single-genome templates, along with the determination of the fraction of cells within the community that encoded them. Subsequent retrieval of PCR products from individual chambers allowed sequence analysis of both genes.

Phylogenetic analysis of the rRNA gene allows classification of the host bacterium, and the metabolic gene is sequenced to confirm that the cell carried the genotype of interest. Additional-

ly, because microfluidic digital PCR yields fluorescent signal upon amplification of a gene regardless of the number of copies present in the cell, this approach can yield estimates of the fraction represented by a given species within the general microbial community. The number of *rnm* operons present in a genome can vary widely, ranging from 1 [e.g., *Rickettsia prowazekii* (19)] to 15 [e.g., *Clostridium paradoxum* (20)], confounding the interpretation of traditional environmental gene inventories. Moreover, the use of single-cell PCR to prepare clone libraries avoids complications and PCR artifacts such as amplification biases and unresolvable chimeric products (21).

We used this technique to examine a complex, species-rich environment: the lignocellulose-decomposing microbial community resident in the hindguts of wood-feeding termites. Therein, the bacterial metabolism known as CO₂-reductive homoacetogenesis is one of the major sources of the bacterial fermentation product acetate (22). Acetogenic bacteria must compete for hydrogen with *Archaea* that generate methane, a potent greenhouse gas for which termites are considered a small yet significant source. Because of their high rates of bacterially mediated homoacetogenesis, many termites contribute less to the global methane budget than they might otherwise (23). Additionally, acetate serves as the insect host’s major carbon and energy source, literally fueling a large proportion of this mutualistic symbiosis (22, 24, 25). A key gene of the homoacetogenesis pathway encodes formyl-tetrahydrofolate synthetase (FTHFS) (26). Although a diverse inventory of termite hindgut community FTHFS variants already existed (27), the identities of the organisms dominating homoacetogenesis in termites had remained uncertain. Here, with the use of microfluidics, we discovered the identities of a multitude of FTHFS-encoding organisms by determining their specific 16S rRNA gene sequences.

The “clone H group” of FTHFS genotypes corresponds to a large fraction of the sequences collected during an inventory of FTHFS genes present in the termite hindgut environment (27). We designed a specific primer set and a fluorescein-labeled probe capable of on-chip detection and amplification of the genotypes comprising this FTHFS group. We also redesigned broad-specificity “all-bacterial” 16S rRNA gene primers and used a previously published probe (28) to amplify and detect bacterial rRNA genes. Both the all-bacterial 16S rRNA gene and clone H group FTHFS primer-probe sets showed single-molecule sensitivity in multiplex on-chip reactions using purified plasmid or termite gut community DNA. The observed success rate for the amplification of individual genes from single-molecule templates was 48% (fig. S1) (29); thus, the success rate for coamplification of two genes from single-molecule templates is estimated to be about 1 in 5.

¹Division of Biology, California Institute of Technology, Pasadena, CA 91125, USA. ²Materials Research and Education Center, Samuel Ginn College of Engineering, Auburn University, Auburn, AL 36849, USA. ³Department of Bioengineering and Howard Hughes Medical Institute, Stanford University, Stanford, CA 94305, USA. ⁴Environmental Science and Engineering Program, California Institute of Technology, Pasadena, CA 91125, USA.

*To whom correspondence should be addressed. E-mail: jleadbetter@caltech.edu

Freshly collected termite hindgut luminal contents were suspended in a PCR reaction buffer and loaded into a microfluidic device (29). Each microfluidic panel uses micromechanical valves to randomly partition a single PCR mixture into 1176 independent 6.25-nl reaction chambers (Fig. 1). We considered single-cell separation to be achieved when fewer than one-third of chambers showed rRNA gene amplification. Assuming a Poisson distribution of cells, under such conditions 6% of chambers should have contained multiple cells or cell aggregates (30). PCR was carried out on a conventional flat-block thermocycler. Amplification was monitored using 5' nuclease probes to generate a fluorescent signal detected with a modified microarray scanner.

Multiplex PCR amplifications from single cells or cell aggregates were successfully performed using diluted gut contents that had been partitioned on-chip (Fig. 2, left). We found global averages of $1.2 (\pm 0.8) \times 10^8$ total bacterial 16S rRNA gene encoding units and $1.5 (\pm 1.0) \times 10^6$ total clone H group FTHFS gene encoding units per *Zootermopsis nevadensis* termite (31). This suggests that, in *Z. nevadensis*, these particular FTHFS genes are carried by a minority population representing ~1% of gut symbionts. The observed variability of these measurements was not surprising, as the *Z. nevadensis* specimens examined were collected from different colonies and locations and had been maintained in captivity for varying periods of time.

Amplification products were retrieved from reaction chambers via syringe needle and were

reamplified, cloned, sequenced, and analyzed using standard methods. Twenty randomly selected chambers that had amplified only a 16S rRNA gene (and not FTHFS) yielded a diversity of *Endomicrobia*, *Firmicutes*, *Bacteroidetes*, *Proteobacteria*, and *Spirochaetes* ribotypes, as expected on the basis of prior 16S rRNA gene clone libraries (32) (figs. S2 and S3). Two-thirds of chambers positive for FTHFS genes did not amplify 16S rRNA genes when either all-bacterial or termite treponeme-specific rRNA gene primers were used. This amplification success rate is comparable to that observed when purified, single-molecule templates were used (e.g., fig. S1) and remains a target for refinement and improvement in the future.

PCR products were retrieved and analyzed from 28 reaction chambers that coamplified both FTHFS and 16S rRNA genes. In 10 of those reactions, sequence analyses revealed that the FTHFS gene had coamplified with a clade of closely related 16S rRNA gene sequences affiliating with the "termite spirochete cluster" (33) of the genus *Treponema*. Members of this novel clade were never observed in chambers that lacked FTHFS gene amplification. An additional three chambers contained a single FTHFS type and multiple 16S rRNA genotypes, one of which in each affiliated with the above-mentioned group [*Zootermopsis* environmental genomovar (ZEG) 11.4, 10.2, and 10.1]. These latter reactions also contained two additional other *Spirochaetes* (Zn-FG7A and B in Fig. 3) in one chamber, a single γ -*Proteobacterium*

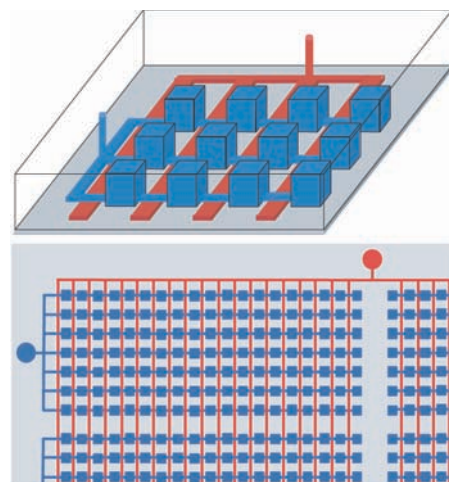


Fig. 1. Microfluidic digital PCR chip. Top: Schematic diagram showing many parallel chambers (blue) connected by channels to a single input. When pneumatic or hydraulic pressure is applied to the control channel network (red), the membranes between the red and blue channels are deflected upward, creating micromechanical valves. When the valves are closed, the continuous blue network is partitioned into independent PCR reactors. Bottom: Schematic showing how a single valve connection can be used to partition thousands of chambers. In the device used, each experimental sample could be partitioned into 1176 chambers, and each device contained 12 such sample panels.

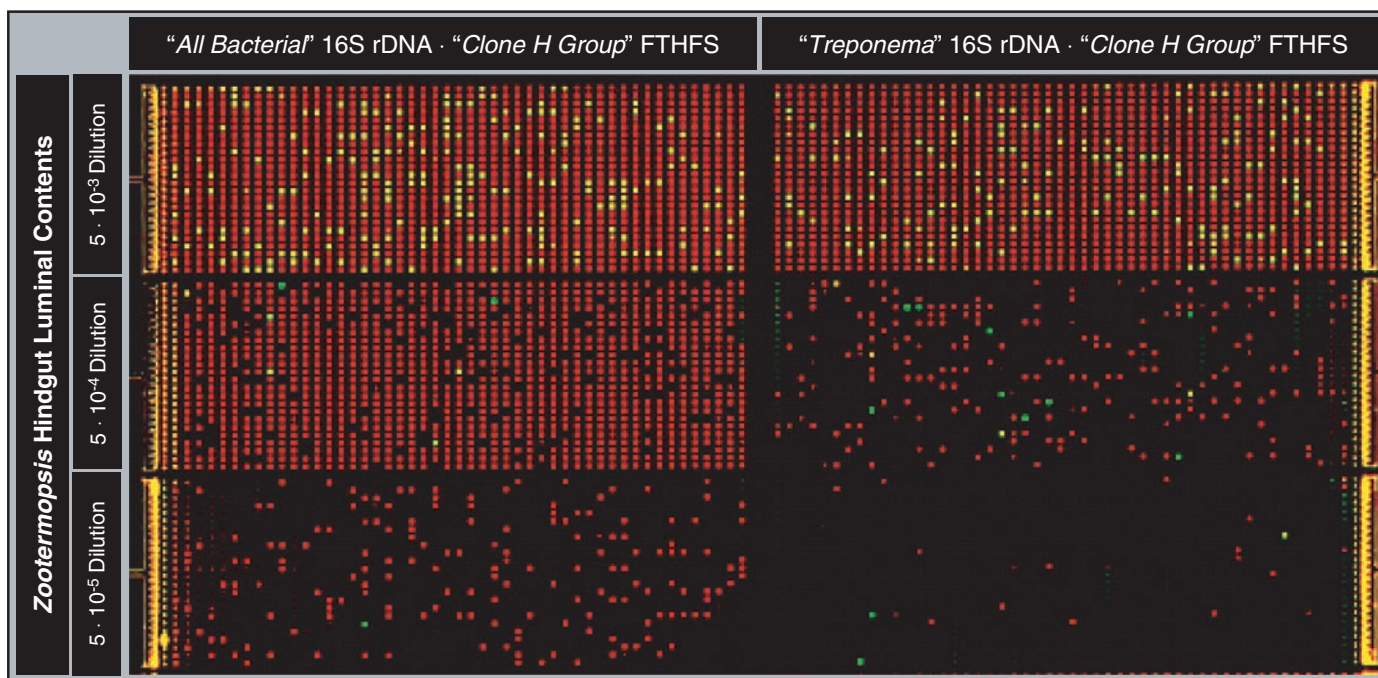


Fig. 2. Multiplex microfluidic digital PCR of single cells in environmental samples. Six panels from a representative experiment show microfluidic digital PCR on diluted hindgut contents harvested from a single *Z. nevadensis* individual. Left: Multiplex PCR using "all-bacterial" 16S rRNA gene (red fluorescence) and "clone H group" (27) FTHFS gene (green fluorescence)

primers and probes. Reaction chambers that contained both genes in 1/500,000 dilutions from this and other on-chip experiments were sampled and the PCR products were analyzed (see Fig. 3). Right: The same, except that 16S rRNA primers specifically targeted members of the "termite cluster" (33) of the spirochetal genus *Treponema*.

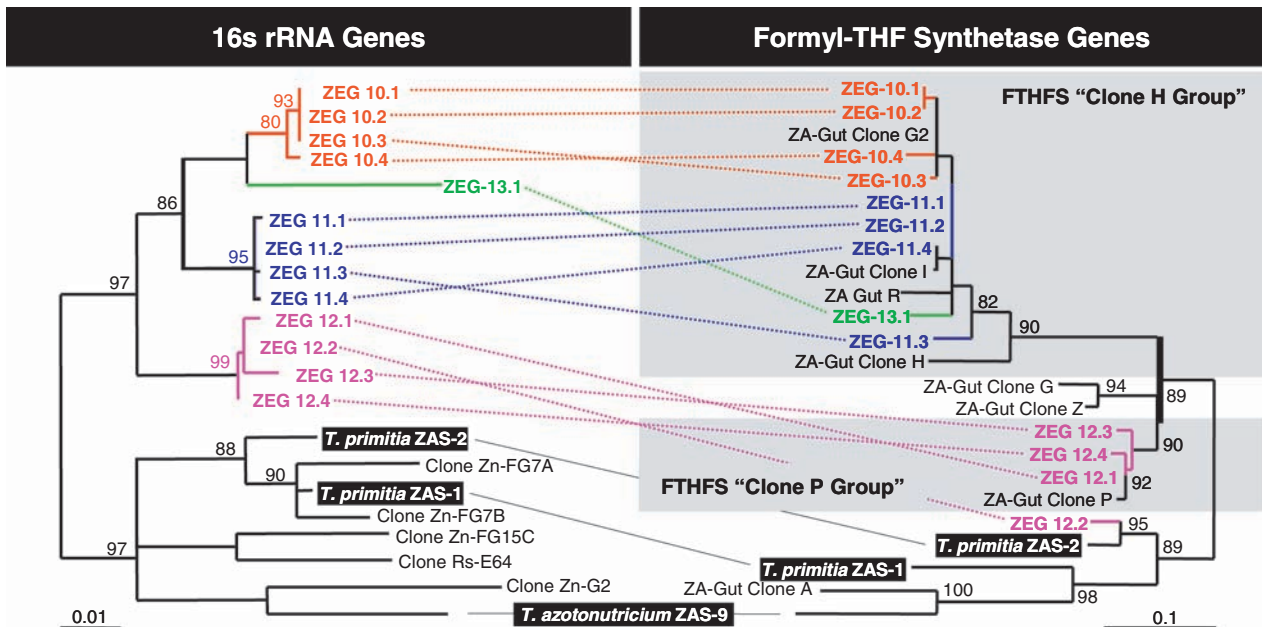


Fig. 3. “Clone H group” and “clone P group” FTHFS genes are encoded by not yet cultivated termite gut treponemes. Left: Phylogenetic tree of 16S rRNA genes cloned from cultivated strain isolates (orange) and from hindgut community microbiota. Right: Phylogenetic tree of FTHFS genes from the termite hindgut. Dotted lines connect genes believed to originate from the same genome. Incongruent gene phylogenies implicate acquisition

of FTHFS genes via lateral gene transfer and can be observed in both isolated species (*Treponema primitia* ZAS-1) and proposed “environmental genomovars” (ZEG 12.2). Scale bars represent substitutions per alignment position. The trees were constructed using TreePuzzle (39); 630 (16S rDNA) and 249 (FTHFS) nucleotide positions were used. Citations for all sequences are listed in table S1.

sequence (Zn-FG12) in the second, and a *Firmicutes* sequence (Zn-FG1) in the third. The remaining 15 chambers analyzed (which coamplified FTHFS and rRNA genes) yielded 16S rDNA sequences in proportions that corresponded well with the ribotype diversity encountered in the general non-FTHFS encoding population. On the basis of this evidence, we conclude that the unique cluster of termite gut treponeme rRNA gene sequences that were repeatedly identified in FTHFS-containing chambers represents the ribotype of the FTHFS-encoding cells. We attribute the instances of FTHFS colocalization with other rRNA gene sequences to cell-cell aggregations. The latter is not to be unexpected in a complex, wood particle-filled, sticky environment such as the termite hindgut (34, 35). Such aggregations appear to be largely random, although there may be a slight enrichment of proteobacterial sequences relative to the general population (figs. S2 and S3). Our results show that FTHFS sequences present in ~1% of bacterial cells were, in 13 of 28 trials, found in association with a 16S rRNA sequence type not identified in 20 random samplings of the bacterial population (16S rRNA-only chambers) at large. The probability of a 16S rRNA gene sequence type that is present in less than 5% of the population randomly colocalizing with FTHFS in 13 of 28 trials is low, on the order of 10^{-10} (36).

Refined phylogenetic analysis of 16S rRNA gene sequences that were repeatedly isolated from FTHFS-containing reaction chambers re-

vealed that all such 16S rRNA gene sequences affiliated within the termite gut treponeme cluster of *Spirochaetes*. These 16S rRNA genes group into four distinct ribotype clusters (Fig. 3). These four sequence types share within-group sequence identity of >99% and between-group identities of 95 to 99%. We propose the term “environmental genomovar” (genome variant) to describe not-yet-cultivated organisms shown to encode two or more known genes of interest. Here, we label the four 16S ribotypes identified as ZEG 10 through 13; three genomovars (ZEG 10, 11, and 13) encode clone H group FTHFS sequences, whereas one genomovar (ZEG 12) encodes a clone P group FTHFS sequence. Previously, nine termite gut treponemes had been isolated and assigned the strain epithet ZAS (*Zootermopsis* acetogenic spirochete) 1 through 9 (37, 38).

To build additional support for a spirochetal origin of clone H group FTHFS genotypes, we designed and used a termite treponeme-specific 16S rRNA gene primer set and gene probe, with the aim of reducing nonspirochetal background (Fig. 2, right). The frequency with which clone H group FTHFS genes were recovered increased from 1 in 175 cells of the general bacterial population, to 1 in 16 treponemal cells [several termite gut treponemes are already known or suspected to encode FTHFS genotypic variants that would not amplify with the clone H group FTHFS primer and probe set (27) (fig. S1)]. Similar to the amplification success rates observed in experiments using the “all-bacterial”

16S rRNA gene primers (Fig. 2, left) and those using the clone H primers against purified single-molecule templates (fig. S1), about one-third of FTHFS-positive reaction chambers also amplified detectable levels of 16S rRNA genes. Treponemal cells were deduced to constitute 10 to 12% of the bacterial community of *Z. nevadensis* (comparing amplification frequencies in the left and right panels of Fig. 3).

Our results show that specific, not yet cultivated *Treponema* species encode variants of a key gene underlying the dominant bacterial metabolism known to affect the energy needs of their termite hosts. The microfluidic, multiplex digital PCR approach taken here can be extended to expand our understanding of the genetic capacities of not-yet-cultivated species, and to collect and collate genetic information in a manner that builds conceptual genomovars that directly represent the organisms catalyzing important activities in various environments of global relevance.

References and Notes

1. N. D. Gray, I. M. Head, *Environ. Microbiol.* **3**, 481 (2001).
2. E. Zuckerkandl, L. Pauling, *J. Theor. Biol.* **8**, 357 (1965).
3. P. Hugenholtz, B. M. Goebel, N. R. Pace, *J. Bacteriol.* **180**, 4765 (1998).
4. S. J. Sogin, M. L. Sogin, C. R. Woese, *J. Mol. Evol.* **1**, 173 (1971).
5. C. S. Riesenfeld, P. D. Schloss, J. Handelsman, *Annu. Rev. Genet.* **38**, 525 (2004).
6. G. W. Tyson *et al.*, *Nature* **428**, 37 (2004).
7. M. Strous *et al.*, *Nature* **440**, 790 (2006).
8. S. G. Tringe *et al.*, *Science* **308**, 554 (2005).

9. J. C. Venter *et al.*, *Science* **304**, 66 (2004); published online 4 March 2004 (10.1126/science.1093857).
10. O. Béjā *et al.*, *Science* **289**, 1902 (2000).
11. J. L. Nielsen, D. Christensen, M. Kloppenborg, P. H. Nielsen, *Environ. Microbiol.* **5**, 202 (2003).
12. M. Manefield, A. S. Whiteley, R. I. Griffiths, M. J. Bailey, *Appl. Environ. Microbiol.* **68**, 2002 (2002).
13. R. I. Amann, W. Ludwig, K. H. Schleifer, *Microbiol. Rev.* **59**, 143 (1995).
14. K. Zwirgmaier, W. Ludwig, K. H. Schleifer, *Mol. Microbiol.* **51**, 89 (2004).
15. K. Zhang *et al.*, *Nat. Biotechnol.* **24**, 680 (2006).
16. B. Vogelstein, K. W. Kinzler, *Proc. Natl. Acad. Sci. U.S.A.* **96**, 9236 (1999).
17. T. Thorsen, S. J. Maerkl, S. R. Quake, *Science* **298**, 580 (2002); published online 26 September 2002 (10.1126/science.1076996).
18. J. W. Hong, S. R. Quake, *Nat. Biotechnol.* **21**, 1179 (2003).
19. H. Pang, H. H. Winkler, *J. Bacteriol.* **175**, 3893 (1993).
20. F. A. Rainey, N. L. Ward-Rainey, P. H. Janssen, H. Hippe, E. Stackebrandt, *Microbiology* **142**, 2087 (1996).
21. S. G. Acinas, R. Sarma-Rupavarm, V. Klepac-Ceraj, M. F. Polz, *Appl. Environ. Microbiol.* **71**, 8966 (2005).
22. J. A. Breznak, J. M. Switzer, *Appl. Environ. Microbiol.* **52**, 623 (1986).
23. A. Brauman, M. D. Kane, M. Labat, J. A. Breznak, *Science* **257**, 1384 (1992).
24. D. A. Odelson, J. A. Breznak, *Appl. Environ. Microbiol.* **45**, 1602 (1983).
25. A. Tholen, A. Brune, *Environ. Microbiol.* **2**, 436 (2000).
26. L. G. Ljungdahl, *Annu. Rev. Microbiol.* **40**, 415 (1986).
27. T. M. Salmassi, J. R. Leadbetter, *Microbiology* **149**, 2529 (2003).
28. M. T. Suzuki, L. T. Taylor, E. F. DeLong, *Appl. Environ. Microbiol.* **66**, 4605 (2000).
29. See supporting material on Science Online.
30. Assuming a Poisson distribution, if 67% of chambers are empty, then the expected number of cells per chamber is $-\ln 0.67$ or 0.40. The probability that a chamber contains more than one cell is $1 - 0.67 - ((e^{-0.40}) * (0.40)^2) / (1)$ or 6.2%.
31. Value ± 1 standard deviation; 13 termites served as source of cells for $n = 32$ sample panels. All sample panels that met our conditions for single-cell separation and contained at least one FTHFS-positive chamber were used in calculation of gut bacterial loads.
32. M. Ohkuma, T. Kudo, *Appl. Environ. Microbiol.* **62**, 461 (1996).
33. T. G. Lilburn, T. M. Schmidt, J. A. Breznak, *Environ. Microbiol.* **1**, 331 (1999).
34. J. A. Breznak, H. S. Pankratz, *Appl. Environ. Microbiol.* **33**, 406 (1977).
35. J. R. Leadbetter, J. A. Breznak, *Appl. Environ. Microbiol.* **62**, 3620 (1996).
36. The binomial distribution function was used to calculate the probability that, in 13 of 28 trials, a sequence that is present in 5% of chambers (0 of 20 16S-only chambers) would randomly colocalize with clone H group FTHFS sequences.
37. J. R. Leadbetter, T. M. Schmidt, J. R. Graber, J. A. Breznak, *Science* **283**, 686 (1999).
38. T. G. Lilburn *et al.*, *Science* **292**, 2495 (2001).
39. H. A. Schmidt, K. Strimmer, M. Vingron, A. von Haeseler, *Bioinformatics* **18**, 502 (2002).
40. We thank M. Unger, A. Daridon, and L. Warren for advice and discussions. Supported by NIH grant 1R01 HG002644-01A1, NIH National Research Service Award grant 5 T32 GM07616, an NIH Director's Pioneer Award, and NSF grant DEB-0321753. S.R.Q. is a founder, shareholder, and consultant for Fluidigm Corporation.

16 June 2006; accepted 30 October 2006
10.1126/science.1131370

Prevention of *Brca1*-Mediated Mammary Tumorigenesis in Mice by a Progesterone Antagonist

Aleksandra Jovanovic Poole,^{1,2*} Ying Li,^{1,2*} Yoon Kim,^{1,2} Suh-Chin J. Lin,^{1,2†} Wen-Hwa Lee,¹ Eva Y.-H. P. Lee^{1,2‡}

Women with mutations in the breast cancer susceptibility gene *BRCA1* are predisposed to breast and ovarian cancers. Why the *BRCA1* protein suppresses tumor development specifically in ovarian hormone-sensitive tissues remains unclear. We demonstrate that mammary glands of nulliparous *Brca1/p53*-deficient mice accumulate lateral branches and undergo extensive alveologenesis, a phenotype that occurs only during pregnancy in wild-type mice. Progesterone receptors, but not estrogen receptors, are overexpressed in the mutant mammary epithelial cells because of a defect in their degradation by the proteasome pathway. Treatment of *Brca1/p53*-deficient mice with the progesterone antagonist mifepristone (RU 486) prevented mammary tumorigenesis. These findings reveal a tissue-specific function for the *BRCA1* protein and raise the possibility that antiprogesterone treatment may be useful for breast cancer prevention in individuals with *BRCA1* mutations.

Mutations in the breast cancer susceptibility gene *BRCA1* are associated with an increased risk of breast and ovarian cancers (1). Reduced *BRCA1* expression due to promoter methylation may contribute to breast cancer progression (2). The *BRCA1* protein has been implicated in DNA damage repair, cell cycle checkpoint control, and transcriptional regulation [reviewed in (3, 4)]. The specific suppression of breast and ovarian

carcinogenesis by the pleiotropic *BRCA1* tumor suppressor has been attributed to its regulation of estrogen receptor α (ER α) and two progesterone receptor isoforms (PRs) (5–8), which play important roles in breast development (9–15). *BRCA1* interacts with ER and PRs directly and modulates ligand-dependent and -independent transcription activities of ER α and PR, as well as nongenomic functions of ER α (5–8). However, the mechanisms by which the ER and PRs contribute to *BRCA1*-mediated carcinogenesis remain unclear.

Hormone replacement therapy with progesterone and estrogen, but not estrogen alone, has been associated with an elevation in breast cancer risk in postmenopausal women (16–18). In mice, the long isoform of PR, PR-B, is required for full development of mammary gland (15, 19), and overexpression of the short isoform, PR-A, leads to abnormal mammary gland

development and ductal hyperplasia (20). These results are consistent with the hypothesis that PRs play a role in breast carcinogenesis.

To address the specific roles of ER and PRs in *Brca1*-mediated tumorigenesis, we studied *p53^{f5&6/f5&6}Cre^c* and *Brca1^{f11/f11}p53^{f5&6/f5&6}Cre^c* mice (fig. S1A) (21, 22). Inactivation of both *Brca1* and *p53* genes in the mouse mammary gland mimics the majority of human *BRCA1*-associated tumors, which also harbor *p53* mutations (3, 4). *Brca1^{f11/f11}p53^{f5&6/f5&6}Cre^c* mammary glands from nulliparous mice at 2.5 months of age showed about 4.5-fold more branching points compared with wild-type or *p53^{f5&6/f5&6}Cre^c* glands (Fig. 1A and fig. S1B). By 4 months of age, the nulliparous *Brca1^{f11/f11}p53^{f5&6/f5&6}Cre^c* mammary gland showed further accumulation of side branches and extensive alveolar formation (Fig. 1B). The mammary gland morphology of mature, nulliparous *Brca1^{f11/f11}p53^{f5&6/f5&6}Cre^c* was similar to that of wild-type pregnant mice, suggesting that proliferation of mammary epithelial cells (MECs) was altered. Proliferation of MECs is regulated by ovarian hormones (23). In the estrous phase, MEC proliferation as measured by 5-bromo-2-deoxyuridine (BrdU) incorporation was about five times higher in the *Brca1^{f11/f11}p53^{f5&6/f5&6}Cre^c* mice than it was in wild-type or *p53^{f5&6/f5&6}Cre^c* mice (Fig. 1C and fig. S1C). Increased MEC proliferation in *Brca1^{f11/f11}p53^{f5&6/f5&6}Cre^c* mice was also seen in the diestrous phase (Fig. 1C and fig. S1C). Previous studies have shown that progesterone exerts its functional effects through paracrine action (24). Indeed, BrdU-positive MECs were found adjacent to PR-positive cells; there were also BrdU and PR double-positive MECs in the hyperplastic *Brca1^{f11/f11}p53^{f5&6/f5&6}Cre^c* mammary gland (fig. S2), indicating that the paracrine action of PR was maintained, at least in most cases.

To assess the contribution of circulating estrogen and progesterone on MEC proliferation,

¹Department of Biological Chemistry, University of California, Irvine, CA 92697–4037, USA. ²Department of Developmental and Cell Biology, University of California, Irvine, CA 92697–4037, USA.

*These authors contributed equally to this work.

†Current address: Division of Developmental Biology, Cincinnati Children's Hospital Research Foundation, Cincinnati, OH 45229, USA.

‡To whom correspondence should be addressed. E-mail: elee@uci.edu